Supplementary Material

Commercial Fibre Products Derived Free-standing Porous Carbonized-Membranes for Highly Efficient Solar Steam Generation

Xiaofeng Lin, Meijia Yang, Wei Hong*, Dingshan Yu*, Xudong Chen*

*** Correspondence:** Corresponding Author: yudings@mail.sysu.edu.cn; hongwei9@mail.sysu.edu.cn; cescxd@mail.sysu.edu.cn;

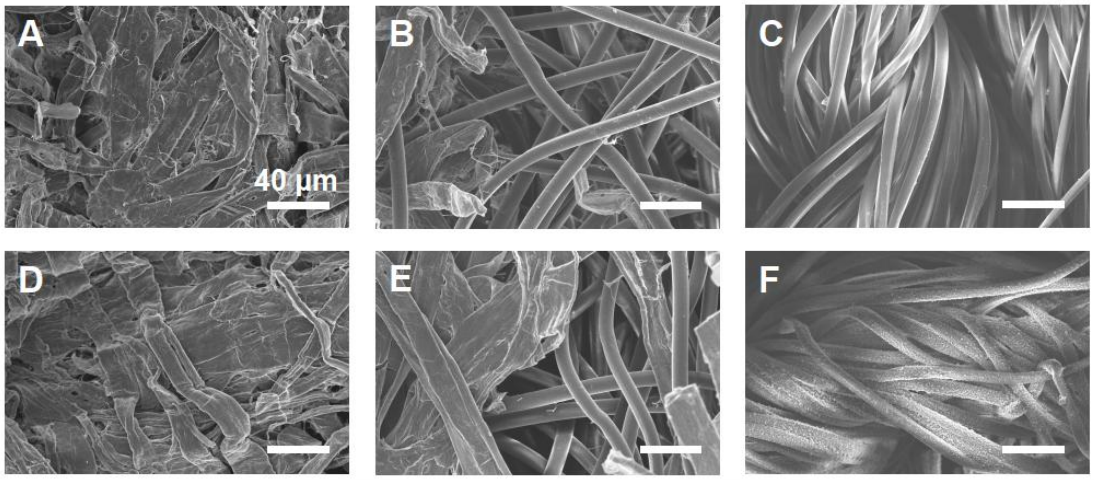

Supplementary Figure S1. The SEM images of the A) CPs, B) APs, C) CWs, D) CCPs, E) CAPs, F) CCWs. Scale bar: 40 μm.

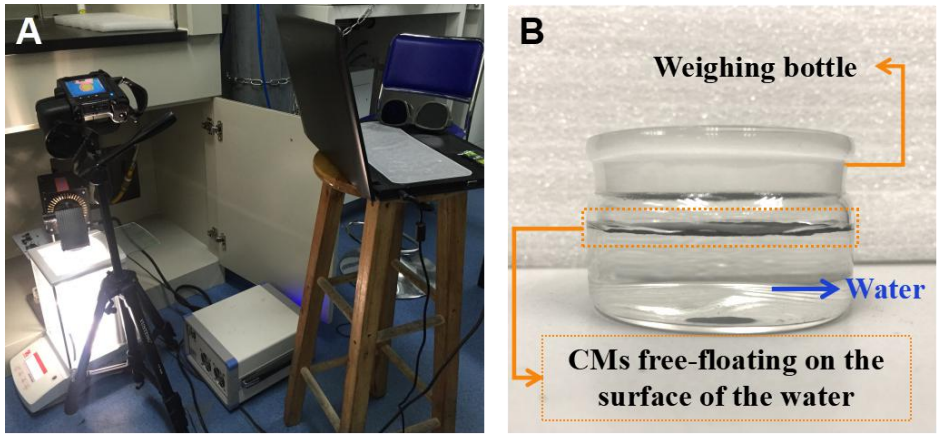

Supplementary Figure S2. A) The photograph of the test system for energy conversion efficiency (η_{ECE}). B) The photograph of a free-floating CMs on the water contained in a weighing bottle.

Supplementary Table S1. Calculation results of the energy conversion efficiency (η_{ECE}).

Samples	$\dot{m}$ (kg·m^{-2}·h^{-1})	Temperature T (℃)	C × (T − T$_0$) (kJ·kg^{-1})	Δh_{vap} (kJ·kg^{-1})	η_{ECE} (%)	Thermal conductivity (W·m^{-1}k^{-1})	Grammage (g·m^{-2})
Pure water	0.431	29.3	17.974	2431.3	29.3	0.56	-
Au-APs	0.856	39.2	59.356	2407.8	58.7	0.49	-
APs	0.440	30.0	20.9	2430.0	30.0	0.124	58.74
CAPs	0.924	40.3	63.954	2405.1	63.4	0.043	80.05
CPs	0.438	29.7	19.646	2430.4	29.8	0.119	20.96
CCPs	0.959	41.2	67.716	2403.0	65.8	0.031	25.45
CWs	0.440	29.9	20.482	2429.9	29.9	0.150	91.65
CCWs	0.722	37.5	52.25	2411.8	49.4	0.058	116.08

The equation for calculating energy conversion efficiency is $\eta_{ECE} = \dot{m}h_{LV}/C_{opt}P_0$. Among the variable parameters, the total enthalpy of liquid-vapor phase change (h_{LV}) contains two parts, which is the sensible heat and the enthalpy of vaporization ($h_{LV} = C \times (T - T_0) + \Delta h_{vap}$). T_0 is the initial temperature of water (25 ℃). T is the vapor temperature measured by the IR camera (details in Table S1). In the temperature ranging from 25 to 50 ℃, the value of C (specific heat capacity of water) is considered as a constant of 4.18 J·g^{-1}·K^{-1}. Meanwhile, Δh_{vap} (the enthalpy of vaporization) is dependent on the temperature, which can be searched from the specialized database.[S1,S2]

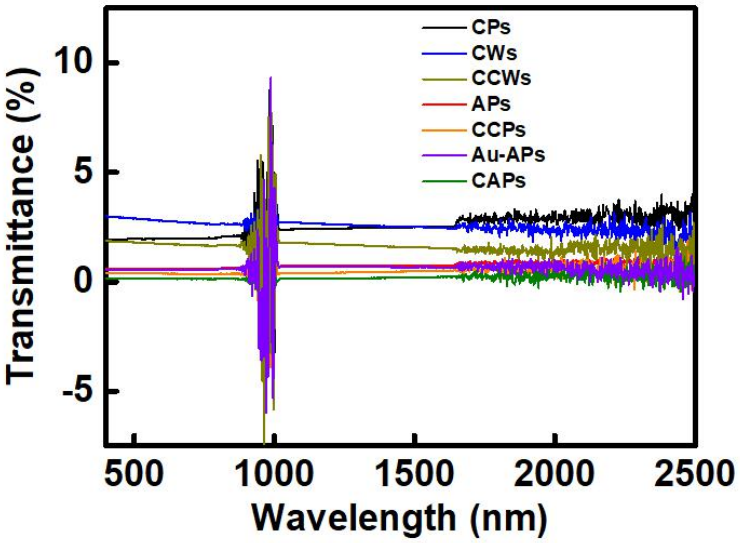

Supplementary Figure S3. The transmittance spectra of Au-APs, APs, CAPs, CPs, CCPs, CWs and CCWs.

Supplementary Table S2. The reflectance, transmittance and absorption of the various samples.

Samples	Reflectance (%)	Transmittance (%)	Absorption (%)
Au-APs	15.36	0.57	84.06
APs	65.44	0.76	33.80
CAPs	8.39	0.19	91.42
CPs	53.03	2.52	44.45
CCPs	7.34	0.45	92.20
CWs	70.33	2.50	27.17
CCWs	27.57	1.57	70.86

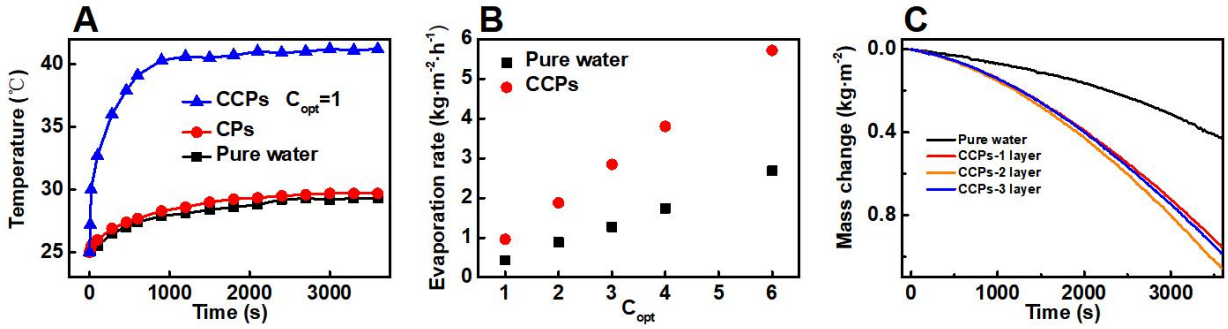

Supplementary Figure S4. A) The typical curves of the interfacial temperature versus time for pure water, CPs and CCPs (floating on the water surface) under solar illumination with a power density of 1 $kW \cdot m^{-2}$. **B)** The average evaporation rates with CCPs (red circular points) and pure water (black square points) under the adjusted solar illumination of 1, 2, 3, 4 and 6 sun. **C)** The typical curves of the mass change versus time for pure water and CCPs with various layers (1, 2 and 3).

Supplementary Table S3. The results of elemental analysis for APs, CAPs, CPs, CCPs, CWs and CCWs

Samples	C (wt %)	H (wt %)	S (wt %)	O (wt %, calculated)
APs	51.88	5.19	0	42.93
CAPs	52	4.35	2.31	41.34
CPs	40.78	5.72	0	53.5
CCPs	49.31	4.25	3.26	43.18
CWs	62.38	4.27	0	33.35
CCWs	56.97	4.23	0.69	38.11

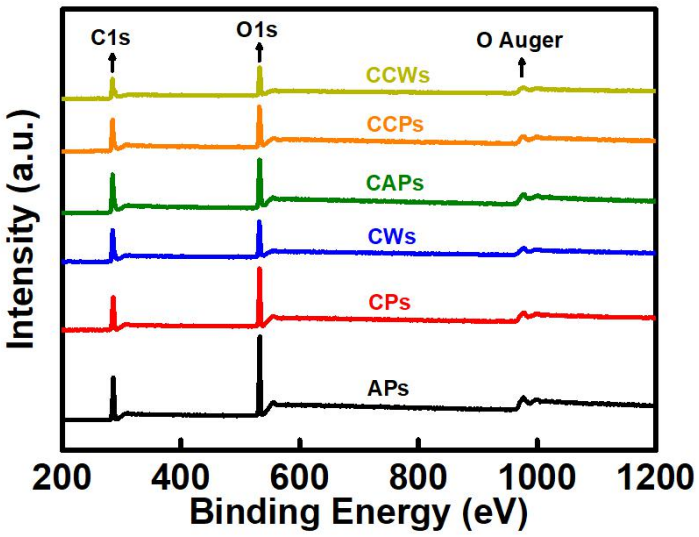

Supplementary Figure S5. Wide-survey XPS spectra of the APs, CAPs, CPs, CCPs, CWs and CCWs.

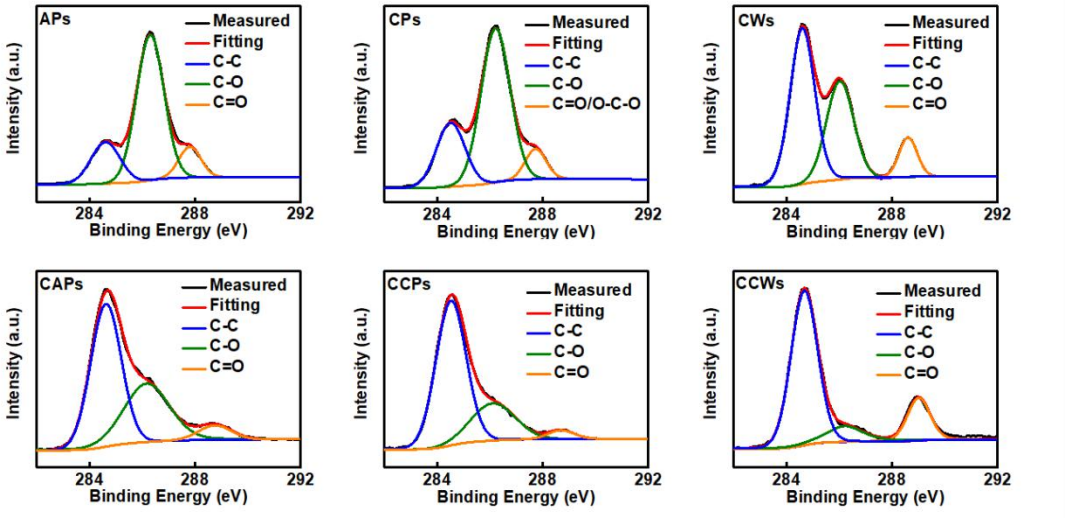

Supplementary Figure S6. The C 1s XPS spectra of the APs, CAPs, CPs, CCPs, CWs and CCWs. The C 1s spectra were divided into several peaks that were fitted by the Gaussian function.

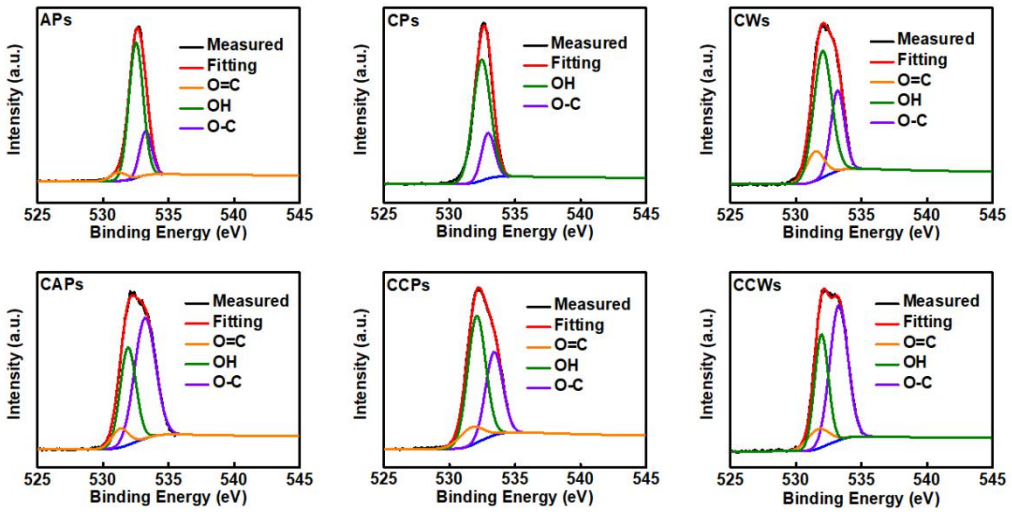

Supplementary Figure S7. The O 1s XPS spectra of the APs, CAPs, CPs, CCPs, CWs and CCWs. The O 1s spectra were divided into several peaks that were fitted by the Gaussian function.

Figure S5-7 have shown the X-ray photoelectron spectroscopy (XPS) spectra of the APs, CAPs, CPs, CCPs, CWs and CCWs. The wide-survey spectra (**Figure S5**) presented two characteristic peaks of C 1s at 284.8 (or 286) eV, O 1s at 532.4 eV and one auger peaks of O. The full-range XPS spectra indicated the presence of carbon and oxygen elements from the APs, CAPs, CPs, CCPs, CWs and CCWs, which corresponded to the composition of cellulose and polyetser contained in the commercial CMs. The **Figure S6** exhibit the high-resolution C 1s spectra of the APs, CAPs, CPs, CCPs, CWs and CCWs, respectively. As can be seen, the C 1s spectra could be divided into three component peaks, which were ascribed to the C–C (284.5~284.7 eV), C–O (286.2~286.3 eV), C=O/O-C-O (287.7~288.1 eV) (or O-C=O (288.6~289.0 eV)), respectively. In the C 1s spectra, the C-C content of the CMs increased apparently compared with the original fibre products, which implied the improvement of the carbonized degree. The high-resolution O 1s spectra in the range of 525-545 eV (**Figure S7**) comprised three peaks, corresponding to O=C (531.2 eV), C-OH (532.0~532.5 eV) and O-C (533.0~533.4 eV), respectively. The content of the O-C and O=C was obviously enhanced in contrast to the C-OH, which also certificated the increase of the carbonized degree of the CMs compared with the original fibre products. Additionally, the elemental analysis further confirmed that the content of the carbon in CAPs and CCPs was higher than those of APs and CPs. Simultaneously, the oxidation degree of the CCWs was enhanced compared with the CWs. As a result, these results indicate that the CMs further increased the carbonized degree and oxidation degree, thereby leading to lower thermal conductivity (see in **Table S1**).

Table S4. The concentrations of Al^{3+}, Fe^{3+}, Cr^{3+}, Cu^{2+}, Mn^{2+} and Ni^{2+} of the ultrapure water, CCPs, CAPs, CCWs, ultrapure water with the CCPs' dipping, ultrapure water with the CAPs' dipping, and ultrapure water with the CCWs' dipping measured by ICP-AES.

Ions	Al^{3+} [mg·L^{-1}]	Fe^{3+} [mg·L^{-1}]	Cr^{3+} [mg·L^{-1}]	Cu^{2+} [mg·L^{-1}]	Mn^{2+} [mg·L^{-1}]	Ni^{2+} [mg·L^{-1}]
Ultrapure water	Lower than the detection limit	Lower than the detection limit	Lower than the detection limit	Lower than the detection limit	Lower than the detection limit	Lower than the detection limit
CCPs	0.12	0.111	0.007	Lower than the detection limit	Lower than the detection limit	Lower than the detection limit
CAPs	0.154	0.144	0.002	Lower than the detection limit	Lower than the detection limit	Lower than the detection limit
CCWs	0.068	0.094	0.007	Lower than the detection limit	Lower than the detection limit	Lower than the detection limit
Ultrapure water with the CCPs' dipping	Lower than the detection limit	Lower than the detection limit	Lower than the detection limit	Lower than the detection limit	Lower than the detection limit	Lower than the detection limit
Ultrapure water with the CAPs' dipping	Lower than the detection limit	Lower than the detection limit	Lower than the detection limit	Lower than the detection limit	Lower than the detection limit	Lower than the detection limit
Ultrapure water with the CCWs' dipping	Lower than the detection limit	Lower than the detection limit	Lower than the detection limit	Lower than the detection limit	Lower than the detection limit	Lower than the detection limit

We have chosen six major trace metals (Fe, Al, Cr, Cu, Mn and Ni), which are probable in commercial products. And we additionally measured the ions concentrations of Fe^{3+}, Al^{3+}, Cr^{3+}, Cu^{2+}, Mn^{2+} and Ni^{2+} via inductively coupled plasma atomic emission spectrometry (ICP-AES, **Table S4).** The results showed that the CMs had very few contents of the Al^{3+} Fe^{3+}, and Cr^{3+}compared with the ultrapure water. Moreover, the CMs have been dipped into the ultrapure water for more than one hour. Then, the ultrapure water with the CMs' dipping was also measured without any the trace metals via the ICP-AES. 0.0145 g CCPs, 0.0285 g CAPs and 0.05 g CCWs were digested with 5 mL HNO_3 (68 wt%), respectively , and diluted to 50 mL with ultrapure water. After calculation from the results of the ICP-AES, the content of the Al^{3+} Fe^{3+} Cr^{3+} in CCPs were 0.0087 %, 0.0080 % and 0.0005 %. The content of the Al^{3+} Fe^{3+} Cr^{3+} in CAPs were 0.0219 %, 0.0205 %, 0.0003 %. The content of the Al^{3+} Fe^{3+} Cr^{3+} in CCWs were 0.0170 %, 0.0235 %, 0.0018 %. When all the CMs were in the same scale (4π cm^2 in the testing of the solar steam generation), the mass of the Al in CCPs, CAPs and CCWs were 0.28×10^{-5} g, 2.21×10^{-5} g, and 2.48×10^{-5} g, respectively. Similarly, the mass of the Fe in CCPs, CAPs and CCWs were 0.26×10^{-5} g, 2.06×10^{-5} g and 3.42×10^{-5} g, respectively. And the mass of the Cr in CCPs, CAPs and CCWs were 1.62×10^{-7} g, 2.86×10^{-7} g and 2.55×10^{-6} g, respectively. From the aforementioned data, we think the content of the trace metals were too low to obtain the relationship between the metal ion conc. and the solar steam conversion activity. The change law of the trace metals among the CMs is not very apparent.

Reference:

S1 a) Dortmund Data Bank Software & Separation Technology, DDBST GmbH, Oldenburg 2016. b) National Institute of Standards and Technology, NIST, Gaithersburg 2017.

S2 Z. Liu, H. Song, D. Ji, C. Li, A. Cheney, Y. Liu, N. Zhang, X. Zeng, B. Chen, J. Gao, Y. Li, X. Liu, D. Aga, S. Jiang, Z. Yu, Q. Gan, Global Challenge 2017, 1, 1600003.